Ecological Modelling 273 (2014) 173–185

Contents lists available at ScienceDirect

Ecological Modelling

journal homepage: www.elsevier.com/locate/ecolmodel

Phenology and density-dependent dispersal predict patterns of mountain pine beetle (*Dendroctonus ponderosae*) impact

James A. Powell[a,b,*], Barbara J. Bentz[c]

[a] Department of Mathematics & Statistics, Utah State University, Logan, UT 84322-3900, United States
[b] Department of Biology, Utah State University, Logan, UT 84322-3900, United States
[c] USDA Forest Service Rocky Mountain Research Station, Logan, UT 84321, United States

ARTICLE INFO

Article history:
Received 20 August 2013
Received in revised form 25 October 2013
Accepted 29 October 2013

Keywords:
Bark beetle
Motility
Temperature
Phenology
Ecological diffusion
Outbreak pattern

ABSTRACT

For species with irruptive population behavior, dispersal is an important component of outbreak dynamics. We developed and parameterized a mechanistic model describing mountain pine beetle (*Dendroctonus ponderosae* Hopkins) population demographics and dispersal across a landscape. Model components include temperature-dependent phenology, host tree colonization determined by an Allee effect, and random-walk dispersal with motility conditioned by host tree density. The model was parameterized at a study site in central Idaho, United States (US), and evaluated at an independent site in northern Washington, US. Phloem and air temperatures, MPB spatial impact data from USDA Forest Service aerial detection surveys, and remotely sensed host tree density data were used to parameterize the model using a maximum likelihood approach. At both study sites the model was highly accurate (>84%) in predicting annual pattern formation when the model was re-initiated each year with the location of new patches of infested trees. Prediction of annual population growth at both sites was also good (>90%), although the model under-predicted area impacted at the Washington site, and at both sites was unable to predict initiation of new small patches. Our model extends previous research by providing a mechanistic description of the link between motility, dispersal and temperature-dependent MPB phenology.

1. Introduction

Dispersal is a key process that connects local population dynamics with patterns at larger spatial scales across a landscape. Dispersal consists of short- and long-distance movement of individuals away from an original source (Nathan et al., 2003). For organisms with irruptive population behavior, dispersal is a key element in population outbreak dynamics (Bjornstad et al., 2002; Aukema et al., 2008). Integrating across temporal and spatial scales is inherently complex, however, and processes that influence dispersal and resultant landscape patterns are unclear for many well-studied species. The mountain pine beetle (MPB) (*Dendroctonus ponderosae* Hopkins, Coleoptera: Curculionidae, Scolytinae) is an economically and ecologically important native species that has caused significant mortality in *Pinus* forests across the western United States and Canada (Meddens et al., 2012). Rapid population growth and inherent positive feedbacks are hallmarks of this species (Raffa et al., 2008). Due to its economic impact, there is an impressive amount of scientific information on MPB, yet the connection of processes at local and large spatial scales and their role in population outbreak dynamics remains unclear (Logan et al., 1998).

Unlike many phytophagous insects, successful MPB reproduction almost always results in death of all or part of the host. Rather than a passive response, host trees have evolved varying defense structures and resin response mechanisms that reduce vulnerability to attack by bark beetles and their fungal and bacterial associates (Boone et al., 2013; Kane and Kolb, 2010; Raffa et al., 2012). There is a density-dependent influence, however, on the effectiveness of host-tree defenses against attack. Vigorous, well-defended trees require rapid attack and colonization by a large number of beetles (i.e., a mass attack) that outpace tree response (Berryman et al., 1985). Conversely, trees stressed by biotic and abiotic agents have a reduced capacity for defense and can be easily overcome by low numbers of beetles (Raffa et al., 2005). The better defended, more vigorous trees tend to be larger and have higher nutritional quality thereby leading to a positive feedback as beetle population density increases (Boone et al., 2011). Like other ectotherms, developmental timing that results in synchronous MPB emergence and increased likelihood of mass attack is a direct result of temperature (Safranyik et al., 1975; Bentz et al., 1991), among other factors. On a given tree, peak MPB attacks that are responsible for death of

* Corresponding author at: Department of Mathematics & Statistics, Utah State University, Logan, UT 84322-3900, United States.
E-mail addresses: jim.powell@usu.edu (J.A. Powell), bbentz@fs.fed.us (B.J. Bentz).

0304-3800/$ – see front matter © 2013 Elsevier B.V. All rights reserved.
http://dx.doi.org/10.1016/j.ecolmodel.2013.10.034

an individual tree can occur within a few days (Bentz et al., 1996), although emergence from multiple trees within a stand can happen over an extended time period, providing sufficient beetles to mass attack multiple well-defended host trees in a localized area (Bentz et al., in press).

The numerous outbreaks across a broad latitudinal and elevational gradient in western North America the past 100–150 years (Alfaro et al., 2004; Evenden and Gibson, 1940; McGregor, 1978; Meddens et al., 2012; Perkins and Swetnam, 1996) highlight the role of adaptation to local thermal regimes in MPB success (Bentz et al., 2011). The severity and distribution of some recent outbreaks, however, differ from what can be inferred from historical records. Moreover, despite the expansive range of MPB, suitable pine hosts extend to the north and south of the current distribution, and range expansion in northern latitudes is ongoing (Cullingham et al., 2011). Increasing temperature associated with climate change is believed to be a significant factor in recent outbreaks and range expansion, with positive influences on development timing and cold survival (Logan and Powell, 2001; Sambaraju et al., 2012). Process-based models describing the effect of temperature on bark beetle developmental timing and survival have been developed (Safranyik, 1978; Bentz et al., 1991; Gilbert et al., 2004; Preisler et al., 2012; Régnierè and Bentz, 2007; Régnière et al., 2012), and have been used to analyze MPB population response to historic and future climate regimes (Bentz et al., 2010; Safranyik et al., 2010). Powell and Bentz (2009) combined temperature-driven phenology, controlling adult emergence timing, with a daily threshold number of beetles required to overwhelm defenses of new host trees under attack (i.e., Allee effect) to produce a model for predicting local population growth rate within a watershed. Using observed phloem temperatures to drive their mechanistic model, year-to-year details of population growth rates and the transition from incipient to epidemic levels of MPB were predicted. The model provides an accurate description of MPB population growth through time, yet the spatial behavior of MPB population spread remains undescribed.

Proliferation of small spots of infested trees is largely dependent on short-range movement under the stand canopy that is conditioned by host tree availability and size, MPB population levels, weather, and behavior-modifying chemicals (Mitchell and Preisler, 1991; Safranyik et al., 1992). Through a chemically mediated synergistic reaction with host defensive compounds, MPB release aggregation pheromones that attract additional beetles (Pitman, 1971; Hughes, 1973) resulting in a mass attack on a single focus tree. Individual trees are finite resources that can be overexploited, however, and a complex suite of derived compounds and behaviors have evolved to redirect attacking beetles to nearby trees (Borden et al., 1987; McCambridge, 1967; Bentz et al., 1996). The combination of self-focusing and self-dissipating forces results in an Allee effect whereby success is enhanced by increasing density at low population levels (Logan et al., 1998). Given appropriate temperature, host trees, and a sufficiently well-synchronized emergence this mechanism can result in spot proliferation (Geiszler et al., 1980).

Safranyik et al. (1989) developed an empirical approach to predict the directional distribution of MPB responding to semiochemicals given wind direction, speed and temperature as it influences MPB emergence. A spatially explicit model describing host tree switching based on similar variables was developed by Powell et al. (1996), parameterized using the spatio-temporal pattern of attacked trees in a stand (Biesinger et al., 2000), and used in an analysis to test hypotheses of MPB outbreak ecology (Logan et al., 1998). These modeling exercises support the notion that higher local host density, which minimizes pheromone plume dispersion, reduces wind, and promotes successful switching to nearby hosts, positively influences outbreak propensity. Given the vagaries of plume dynamics and micrometeorology, however, it is unlikely that a mechanistic model for MPB dispersal including chemotactic details can be predictive.

Ignoring the effects of behavior-modifying chemicals, Heavilin and Powell (2008) fit deterministic integrodifference equation models to data describing spatial patterns of MPB killed trees. The models incorporated possible Allee effects using type III functional responses and described MPB dispersal via Gaussian and exponential dispersal kernels (Heavilin et al., 2007). The models predicted that mean dispersal distances were between 15 and 50 m, a finding similar to other studies (Safranyik et al., 1992; Robertson et al., 2007), although no parameters tested reconciled predictions with observed spatial pattern at any scale. More than three quarters of attacks on new trees occur within 100 m (Robertson et al., 2007), but a significant aspect of MPB dispersal is long distance movement (>2 km, Robertson et al., 2009). At least some of this movement occurs above the canopy (de la Giroday et al., 2011), and localized infestations can irrupt in areas geographically disjunct from other spots (Aukema et al., 2006). Empirical models (Aukema et al., 2008) clearly indicate that longer-range dispersal, linked with temperature, is necessary to understand mountain pine beetle outbreak progression. However, a mechanistic description of how temperature and dispersal control MPB population spread in space and time does not exist.

The goal of our study was to develop a mechanistic model for MPB outbreak dynamics incorporating three simple mechanisms: (1) effects of temperature on adult emergence distribution, (2) random-walk dispersal conditioned on local host density, and (3) an Allee effect requiring MPB attack density to exceed a specified tree defensive threshold for successful colonization of a host tree. The dispersal model reflects three basic assumptions about beetle movement:

- Beetles can effectively focus their attacks on individual hosts to exceed defensive threshold within a small area (~10 m).
- At larger scales beetle movement rates are conditioned on local density of host trees. That is, probability of leaving a stand depends directly (and inversely) on the density of live hosts in the stand. Beetles move rapidly through areas with sparse host trees and slowly where host trees are dense. We assume there is no response to landscape-scale gradients of behavior-modifying chemicals.
- Dispersal occurs on a diurnal cycle; MPB either successfully disperse and attack new hosts or die within a relatively short (daily) time period.

At a population level, such a model amounts to 'ecological diffusion' (Turchin, 1998), in which the probabilities of individuals leaving a patch (i.e., a stand of host trees) is proportional to the 'motility'. Turchin's motility is inversely related to residence time per area of habitat and (equivalently) inversely related to the resistance of a patch to beetle movement. In the case of MPB motility we assumed that motility is strongly conditioned by local host density. We constructed our ecological diffusion model using motilities that decrease exponentially with host density, reflecting increasing residence time for beetles within a patch when there are more hosts to sample. Conversely, residence times will be short (small resistance to movement) in patches with few or no hosts, allowing for relatively rapid and longer-distance dispersal.

We review a phenology model linking hourly temperatures and MPB emergence distribution with an Allee effect for successful host colonization (Powell and Bentz, 2009), then present an ecological diffusion model describing MPB dispersal that is dependent on host tree density. The coupled models were parameterized using maximum likelihood and host tree density, spatial MPB impact data and temperature data from a study area in central Idaho. Since the

maximum likelihood approach required frequent, fine-scale, computationally intensive integration of the coupled models, we used a homogenization approach to accelerate solutions by six orders of magnitude while maintaining accuracy. The model was evaluated using host tree density, spatial MPB impact data and temperature data from an area with recent MPB activity in northern Washington. Results, assessed by spatial correlation, growth rate comparison and confusion matrices, indicate that although the model missed initiation of small spots of infested trees each year, more than eighty percent of the observed pattern of total impact at the landscape scale was captured.

2. Methods

2.1. Study areas

2.1.1. SNRA study area

The Sawtooth National Recreation Area (SNRA) in central Idaho was chosen as our study area for several reasons. A single host, lodgepole pine (*Pinus contorta* Douglas), predominates and grows in stands with relatively homogenous demographics at the lowest elevations. Lodgepole pine stands in the SNRA are within a coherent geographic unit, bounded by 3000+ m mountains on three sides, minimizing factors such as immigration that have been shown to be important in MPB outbreaks (Aukema et al., 2008). The landscape is characterized by a valley and surrounding mountains. The valley opens to the north, cross-wise to prevailing weather patterns, and is small enough that the entire valley experiences the same general climate.

The study area is a rectangular region from approximately 44°22′ N to 43°44′ N (~60 km) and 115°10′ W to 114°28′ W (~30 km), comprising over 1800 km^2. Elevation ranges from 1651 m to 3605 m; vegetation types range from shrub and grasslands to coniferous forests dominated by Douglas fir (*Pseudotsuga menziesii* (Mirb.) Franco), subalpine fir (*Abies lasiocarpa* [Hook.] Nutt), and lodgepole pine and whitebark pine (*P. albicaulis* Engelm.). Densities of pine average 450 trees/ha, although the valley includes many dense stands of 1000 trees/ha as well as meadows and pasture land with no hosts. Extensive barren areas exist above tree-line at the highest elevations. The climate is characterized by very cold winters (nighttime temperatures often less than −20 °C) and mild summers (daytime temperatures generally below 25 °C).

Between 1995 and 2005 a MPB outbreak occurred throughout the SNRA study area, impacting more than a third of the pine host type (Pfeifer et al., 2011). Extensive studies on MPB phenology and life history have been conducted within the study area boundary (Bentz and Mullins, 1999; Bentz, 2006; Powell and Bentz, 2009), and populations from this area were used in development of rate curves included in the MPB phenology model.

2.1.2. Chelan study area

For purposes of validation, our modeling approach was applied to observations collected in a novel region. The Chelan study area in northern Washington encompasses over 446,000 ha, from approximately 47°56′ N to 48°35′ N and from 119°52′ W to 120°44′ W. Elevations range from 336 m at Lake Chelan to peaks at 2700 m. The study area is comprised of public and private lands, including portions of the Methow Valley and Chelan Ranger Districts, Okanagan-Wenatchee National Forest, and North Cascades National Park. The Methow River drainage characterizes the eastern half of the study area. Coniferous vegetation within the study area includes ponderosa pine (*P. ponderosa*), lodgepole pine and whitebark pine; Englemann spruce (*Picea englemannii* Parry) and Douglas fir, with host trees averaging 500 trees/ha. The Chelan study area boundary was chosen to encompass pine vegetation susceptible to MPB infestation and active MPB patches based on ground surveys. MPB impact began in the late 1990s and peaked in 2008 (Crabb et al., 2012).

2.2. Pine density data

Spatially explicit datasets of pine density at 30-m resolution were derived for both study areas using existing geospatial datasets of vegetation composition and structure (Crabb et al., 2012). Briefly, for the SNRA study area forest density (trees per hectare >2.54 cm DBH) at 250 m resolution, developed by the USDA Forest Service FIA (Blackard et al., 2008), were downscaled to 30 m resolution using data from the inter-agency Landscape Fire and Resource Management Planning Tools Project (LANDFIRE). Data from the GNNFire project (LEMMA, 2005; Pierce et al., 2009) were used to derive pine density matrices of potential pine hosts for the Chelan study area at 30 m resolutions. Methods for both study areas are described in detail in Crabb et al. (2012).

2.3. Phloem temperature data

The developmental environment of MPB is the phloem of pine trees, which is often significantly warmer than ambient temperatures, particularly on the southern bole aspects due to radiant solar input (Lewis, 2011). In lodgepole pine, northern bole aspect temperatures track ambient temperatures with a short time lag and thermal buffering, although they are occasionally slightly higher than ambient, possibly due to re-radiation of solar energy from the surroundings. MPB develop and emerge on all aspects of a tree equally well (Rasmussen, 1974; Bentz, 2006), although adults that emerge from south bole aspects tend to be smaller (Bentz et al., in press). Phloem temperatures were measured on both northern and southern aspects of the bole at a height of approximately 1.8 m above the ground. Phloem temperature probes consisted of fine-gauge (24 AWG) chromega-constantan thermocouples (OMEGA Engineering, Inc., Stamford, CT) and were connected to a datalogger (Campbell Scientific, Inc., Logan, UT). Air temperature was also recorded in each stand using a Campbell 107 thermister temperature probed mounted in a 6-plate louvered shield. Temperature data was recorded every minute, averaged, and stored for each hour. Continuous records from initiation of attacks on trees to adult emergence 1 and 2 years later were collected.

At the SNRA study area, a total of 12 MPB-infested lodgepole pines at 4 sites were monitored. Temperature data were taken from different infested trees in sequential years forming a continuous thermal record from JD 200 in 1994 to JD 289 in 2004. At the Chelan study area, phloem temperatures of MPB-infested trees were measured for two successive MPB generations between 2009 and 2011. Four trees were monitored each year at three sites within the Chelan area, two in lodgepole pine and one site in whitebark pine (Bentz et al., in press).

Downscaled daily maximum and minimum air temperature predictions, at approximately 6 km spacing, were obtained for the SNRA and Chelan study sites from the Climate Impacts Group (Littell et al., 2011). The downscaled temperature data is based on an ensemble delta method. Thirty-seven downscaled grid points covered the SNRA study area over the time period 2004–2006, and 56 grid points were obtained for the Chelan study area for the time period 1990–2009. Because phloem temperature is often different than ambient air temperatures within a lodgepole pine stand, phloem temperature was predicted from the downscale air temperature measurements using a reverse-bootstrapping approach (Lewis, 2011). Essentially, observed phloem temperatures were used in a look-up table, labeled with the day's ambient maximum and minimum temperatures and the next day's minimum. Phloem temperatures at novel points were selected from the

look-up table using the closest least-square-error match to the local daily min–max–min air temperature signal. For both study sites corresponding predictions of annual phenology were generated at each downscaled temperature grid point using the MPB phenology model. Model output was then distributed across the landscape using a nearest-neighbor approach that associated points on the landscape with closest grid locations using altitude, slope and aspect.

2.4. Aerial detection survey data

Geo-referenced data describing the annual number of MPB-killed trees was obtained for both study areas beginning in 1991 and 1980 for the SNRA and Chelan areas, respectively (USDA Forest Service, www.foresthealth.info/portal). The aerial detection surveys (ADS) are conducted in a fixed-wing aircraft by trained observers that manually record numbers of killed trees based on the color of tree foliage (Halsey, 1998). Foliage of dead, beetle-killed trees changes from green to red within a single year. ADS datasets include 'damage' polygon shapefiles with metadata describing the estimated number of trees per acre affected and a code for the damage causal agent(s) (DCA). Only areas with at least 20 trees per hectare were mapped. These georeferenced data served as our source of information on the spatial location, timing, and intensity of MPB impact in both the SNRA and Chelan study areas.

Polygons depicting MPB impact were queried using their unique DCA code by host tree species. Rasters of total MPB impact by year were created by summing MPB impacts across observations for each polygon, then converting the polygons to rasters. The rasters were produced at a 30 m resolution and kept in the same coordinate system as the original ADS shapefiles, North American Datum (NAD) 1983 Albers for both study areas. All other geospatial raster data used in this study were converted into this projection at 30 m resolution using ArcGIS 9.3 software (ESRI, 2008).

2.5. Predicting phenology from phloem temperatures

MPB complete eight life stages underneath the bark of colonized hosts, and progress in each stage depends directly on temperature (Bentz et al., 1991). As females excavate a nest gallery vertically under the bark they lay approximately 2 eggs/cm, immediately injecting the distribution of ages with several weeks of variance. Eggs hatch in 1–3 weeks and the larvae burrow horizontally, consuming phloem. Individuals molt through four larval instars, after which the larvae excavate a chamber and pupate. Teneral adults then consume sporulating fungi inside the pupal chambers, finishing development and preparing to burrow back out through the bark to seek new hosts one or two years later. Development in each stage proceeds at a rate depending directly on phloem temperatures, and each individual develops at a slightly different rate in each stage, potentially broadening the emergence distribution in time. On the other hand, different life stages have different lower thermal thresholds, mainly increasing in the later life stages (Jenkins et al., 2001). This exerts a synchronizing influence, compressing the emergence distribution as individuals molting from one stage find themselves below threshold in the next stage, allowing slower developers to catch up (Powell et al., 2000).

We used the phenology model developed for MPB by Gilbert et al. (2004), accounting for developmental variability in each stage and driven by developmental rates with stage-specific developmental thresholds and thermal optima (Table 1). Details are presented in Appendix A. The model was driven by south side phloem temperatures, as suggested by Powell and Bentz (2009), but sensitivity to differing thermal inputs was also tested. In the current model we assume that phloem temperatures are the main driver of MPB development rate. We acknowledge that other factors, which may themselves be affected by temperature, can also influence MPB development rate including fungal symbionts (Addison et al., in press), humidity, and parasites and predators (Amman and Cole, 1983).

2.6. Modeling dispersal and attack

The ecological diffusion model,

$$\frac{\partial P}{\partial t} = \left(\frac{\partial^2}{\partial x^2} + \frac{\partial^2}{\partial y^2} \right) [\mu(S)P], \quad (1)$$

was used to distribute dispersing beetles (P) across the landscape. Individuals leave a patch at rate $\mu(S)P$ (Turchin, 1998), where motility ($\mu(S)$) decreases with the density of susceptible hosts (S). Each

Table 1
Variables used in the integrated model predicting the evolution of MPB attack patterns. Hectares denoted by 'ha'.

Variable	Description	Units
Phenology model		
$p_i(a, t)$	Density of MPB at age a in life stage i at time t during development	MPB/(age class)
$T(t)$	Hourly temperature at time t during development	°C
$r_i[T(t)]$	Developmental rate curve in life stage i	1/day
$E_n(j)$	Emerging (adult) MPB on Julian day j of year n	MPB/day
R_n	Population growth rate (discrete) in year n	–
Dispersal and attack model		
$P(x, y, t)$	Density of dispersing MPB at (x, y) at time t during a day	MPB/ha
$S(x, y)$	Density of susceptible (>20 cm DBH) host trees at (x, y)	stems/ha
$\mu(x, y)$	MPB motility at (x, y)	km^2/day
$C(x, y, j)$	Number of colonizing MPB in pixel centered at (x, y) on day j	MPB
$H_n^{obs}(x, y)$	Density of observed red top trees at (x, y), year n	stems/ha
$H_n^{pred}(x, y)$	Density of predicted red top trees at (x, y), year n	stems/ha
MLE approach		
$O_{j,k}^n$	Impacted area observed at error grid location (xe_j, ye_k) in year n	km^2
$I_{j,k}^n$	Impacted area predicted at error grid location (xe_j, ye_k) in year n	km^2
NLL_n	Negative Log Likelihood in year n	–
L	Total likelihood of the parameters given the data	–
Homogenization		
$c(x, y, t)$	Realized MPB motility at (x, y) at time t during a day of dispersal	MPB-days
$\overline{\mu}(x, y)$	Geometric average of motility	km^2/day
$\Omega(x, y)$	Spatial region, centered at (x, y), for calculating geometric average	–
$\|\|\Omega(x, y)\|\|$	Area of the region $\Omega(x, y)$	km^2

Table 2
Parameters used in the integrated model to predict the evolution of MPB attack patterns. Either parameter estimates or nominal parameter values appear as appropriate. Above we denote hectares by 'ha'.

Parameter	Description	Units
Phenology model		
ν_i	Rate of developmental variance increase with time in stage i	1/day
N	Surviving brood per infested tree	MPB
Dispersal and attack model		
μ_0	MPB motility in habitat with no hosts	3.79 km^2/day
μ_1	Exponential rate of decrease of motility with host density	−10.9
N	Brood/infested tree which survive to emergence	2043 MPB/tree
I	Impact; assumed number of infested trees per impacted ha	100 trees/ha
r	Attack Radius	17 m
A	Attack threshold	39.8 MPB
α	Number of trees colonized/successfully attacking MPB	1/698 trees/MPB
Δx	Width of individual pixel in x direction	30 m
Δy	Width of individual pixel in y direction	30 m
MLE approach		
β_1	Maximum number of new infested trees created per pixel	31.0 trees
β_2	Decrement of potential new infested trees imposed by attack threshold	0.067 trees
Δxe	Width of error grid in x direction	0.96 km
Δye	Width of error grid in y direction	0.96 km
σ^2	Variance of error distribution	2.33×10^{-3} km^2

day's emerging MPB in a pixel was proportional to the number of infested trees (H_n^{obs}) and the number of brood per tree (N). Emergence predictions for each day were generated using south side phloem temperatures, following Powell and Bentz (2009). At the end of each day beetles arriving at each pixel contributed to successful attacks based on their probability of exceeding an attack threshold, A, within an attack radius, r, of pixel center. It was assumed that all beetles within this radius could coordinate their efforts to attack any given tree within the pixel; thus, within an area of πr^2 of pixel center all arriving MPB were allowed to collaborate to exceed attack threshold on individual trees in the pixel. At the end of the season all successfully attacking MPB in each pixel were summed over the season and converted into newly attacked trees, H_{n+1}^{pred}, at a rate α trees/MPB. The model was re-initialized each year with ADS observations of the spatial location of new infested trees. Mathematical details of this procedure are presented in Appendix B.

Motility was of the form

$$\mu = \mu_0 \, exp\left[-(\mu_1 + \ln(\mu_0))\frac{S(x,y)}{1000}\right]. \quad (2)$$

This gave a maximum dispersal rate of μ_0 km^2/day when no hosts were present, decreasing exponentially to $e^{-\mu_1}$ in a densely stocked stand with $S = 1000$ trees/ha. Both μ_0 and μ_1 were unknown *a priori*, although it was expected that μ_0 is of order 1–5 km^2/day, accommodating evidence that landscape impacts correlate at scales <10 km (Aukema et al., 2008). By contrast, $e^{-\mu_1}$ was expected to be only tens of squared meters per day, reflecting observations that mean dispersal distance in infested stands is on the order of tens of meters among susceptible hosts (Safranyik et al., 1989; Robertson et al., 2007). The exponential decrease in motility with susceptible host density reflected increasing residence time in more dense stands as MPB search for susceptible hosts or hosts currently under attack (Table 1).

2.7. Estimating parameters using ADS data

Maximum likelihood estimation (MLE) was used to optimize correspondence between observed ADS patterns of MPB-caused tree mortality and model predictions on 0.48 km (sixteen 30 m pixel) blocks. The unknown parameters were μ_0 and μ_1 (describing motility), number of surviving brood per attacked tree (N), density of attacked trees/ha (I) within each ADS pixel, attack radius (r), attack threshold (A), and number of successfully colonizing MPB per new impacted tree ($1/\alpha$). These parameters were not all identifiable; predicted impacts depended on two parameter combinations, $\beta_1 = \pi\alpha r^2 NI$ and $\beta_2 = \alpha A$, as well as the motility parameters μ_0 and μ_1. The four identifiable parameters, μ_0, μ_1, β_1 and β_2, were estimated using MLE; estimates for N and A were determined using reference values for α, r and I consistent with field observation (see Table 2). Details of the likelihood function and optimization procedure are given in Appendix C.

2.8. Accelerating predictions using homogenization

Implementation of the dispersal model as part of an MLE approach was computationally intensive. For each choice of parameters the ecological diffusion model required integration on a 1000×2000 grid of 30 m pixels over nine years. Each year had at least 30 days of peak emergence, which would have required subdivision into 30 s time steps to maintain computational accuracy with maximum motility on the order of 1 km^2/day. However, the ecological diffusion model could readily be homogenized to speed up the computational approach. This procedure used asymptotic techniques to deduce a related, 'homogenized' equation on large spatiotemporal scales. Solutions to the homogenized equation were then projected onto small scales to accurately, but rapidly, provide results at individual pixels. Details of homogenization for ecological diffusion are presented in Garlick et al. (2011), and a summary is in Appendix B. In our case, homogenization allowed computations on scales at least 30 times larger in space and 1000 times larger in time, giving a speed-up of six orders of magnitude.

2.9. Analysis of model performance

Model accuracy was tested in several ways. Growth rates for a given year, used as one measure for model success, were calculated as the ratio of the current year's area impacted with the previous year's area impacted across an entire study area. To assess spatiotemporal predictivity, each study area was divided into 'error' blocks 0.96 km (thirty-two 30 m pixels) on a side, and presence/absence of predicted/observed MPB impact denoted as either one or zero. A confusion matrix was constructed by tallying correct and incorrect predictions across all years. Diagonal elements of the confusion matrix are correct model predictions and off-diagonal elements are either false negatives (lower left) or false

Table 3
Confusion matrix for model predictions, tabulating agreement between model predictions and observations on a grid with cell width 0.96 km across all years of model prediction. Diagonal elements of the confusion matrix are correct model predictions of either MPB impact or non-impact; the off-diagonal elements are either false negatives (lower left) or false positives (upper right). The ratio of correct (diagonal) elements to all elements gives an accuracy of 85.66%.

	Model predicts	
	Non-impacted cell	Impacted cell
Non-impacted cell observed	1786	2001
Impacted cell observed	520	13,270

positives (upper right). The sum of the diagonal elements divided by the total of all elements provides an indication of the percent model accuracy across all pixels and years, reported as model predictivity. Spatiotemporal correlation coefficients were also calculated for the model on the 0.48 km (16 pixel) blocks used for model parameterization (see Appendix C). Each yearly raster of ADS observations and corresponding model predictions were converted to vectors and those vectors concatenated across years. The correlation coefficient between predictions and observations was reported as the model correlation.

2.10. Model sensitivity

To test the robustness of model predictions, simulations were run using ADS, host density and temperature data from the Chelan study area from 1990 to 2009. Model parameters estimated for the SNRA study area were used in model runs (Table 2). Hourly temperature data from 1990 to 2009 were estimated using the downscaled temperature data and reverse-bootstrapping (Lewis, 2011) that was based on observed phloem and air temperature data at 3 sites within the Chelan study area from 2009 to 2011. Model accuracy was tested as described above for the SNRA study area.

To test model sensitivity critical inputs and estimated parameters were altered. Sensitivity to thermal input was tested by using phloem temperatures from the north bole aspect and air temperature, rather than south bole aspect temperatures. The effect of host density was tested by altering tree density of individual pixels. Pixels with host densities >200 trees/ha were replaced with the overall mean density of all pixels, and pixels with <200 trees/ha were replaced with 0. The exponential decrease in motility (μ_1) was reduced by 50%, corresponding to an overall increase in motility in densely stocked patches. The influence of the Allee effect, or the threshold number of emerging beetles required to successfully overcome a tree, was tested by setting A to 0 (i.e., no effect), 10 and 100. The values of 10 and 100 were chosen as reasonable upper and lower credible limits for attacks on individual trees to become self-sustaining, based on observations of attacks on baited trees (Bentz et al., 1996). The number of surviving brood directly influenced how many emerging adults are available to potentially surpass the threshold of attack. Model sensitivity to this variable was tested by reducing the original value by 50% and doubling the original value.

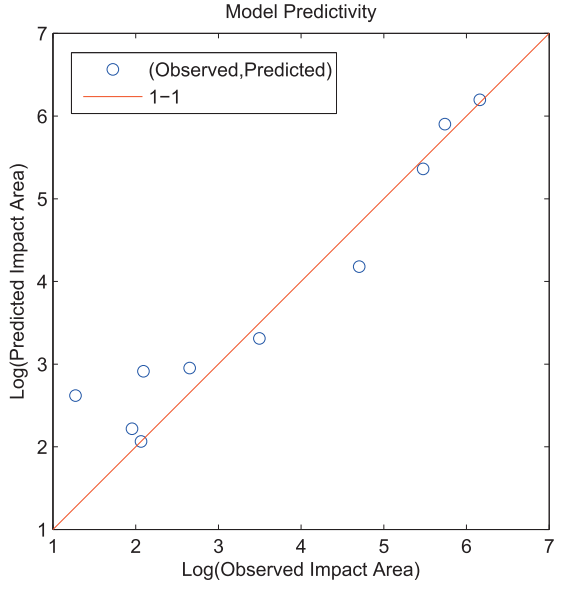

Fig. 1. Comparison of yearly predicted area of impact with observed area of impact in the SNRA on a logarithmic scale. The line of perfect prediction, with slope 1, is indicated; model predictions are indicated as small circles. The more closely the predictions conform to the line the better the model predictivity.

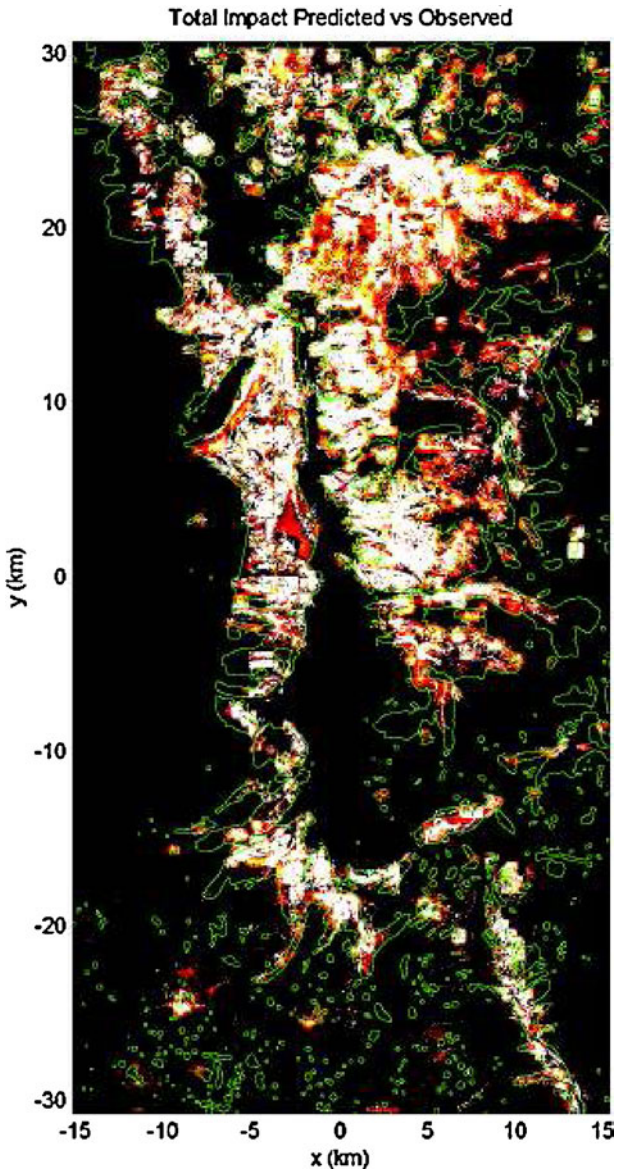

Fig. 2. Density plot of model predictions for the SNRA, summed across years from 1995 to 2003, compared with contours of ADS observations likewise summed across years. Contours of ADS data indicate regions in which ADS observations exceeded one MPB-attacked tree in a 30 m pixel in some year. Model predictions are rendered in a 'hot' colormap with white saturating at 1000 predicted total killed trees per hectare and black indicating no attacked trees in any year. Cell by cell correlation on squares of size 0.9216 km^2 was $r = 0.7502$.

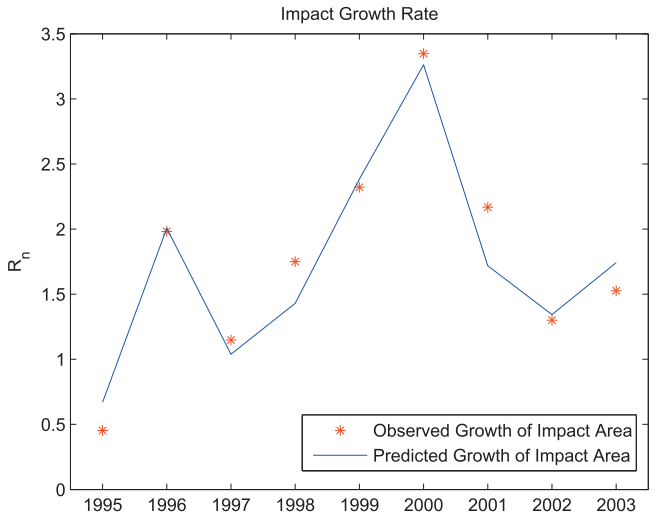

Fig. 3. Comparison of yearly predicted growth rates (solid) with observed growth rates (*) in the SNRA. Growth rates for a given year are diagnosed by computing the ratio of current year's area impacted by MPB with previous year's impacted area.

3. Results

3.1. SNRA study area

MLE parameters are given in Table 2. Robustness of the optima was tested by repeated iteration of the search algorithm for differing initial parameter 'guesses'. The best estimate for unimpeded motility was $\mu_0 = 3.79\,\text{km}^2/\text{day}$, with an associated exponential decrease estimated at $\mu_1 = -10.9/1000$ hosts, corresponding to $\mu = 18.5\,\text{m}^2/\text{day}$ in a pixel stocked with 1000 hosts per hectare. The best estimate for number of surviving brood per infested host was $N = 2043$. This parameter was contingent on the assumption that newly colonized hosts contain $1/\alpha = 698$ female MPB (Powell and Bentz, 2009). If each female produces 80 eggs (Régnière et al., 2012), this equates to a survivorship of 4%, which is reasonable during an outbreak (Safranyik and Carroll, 2006). The daily threshold for successful attack was estimated to be $A = 39.8$ MPB/day per tree, using a 17 m attack radius.

Treating each 0.48 km parameterization block in each year as a binary element (zeros/ones for non-impact/impact by MPB) in separate vectors of predictions and observations, we calculate a correlation coefficient of 0.7502 ($r^2 = 0.563$) between predictions

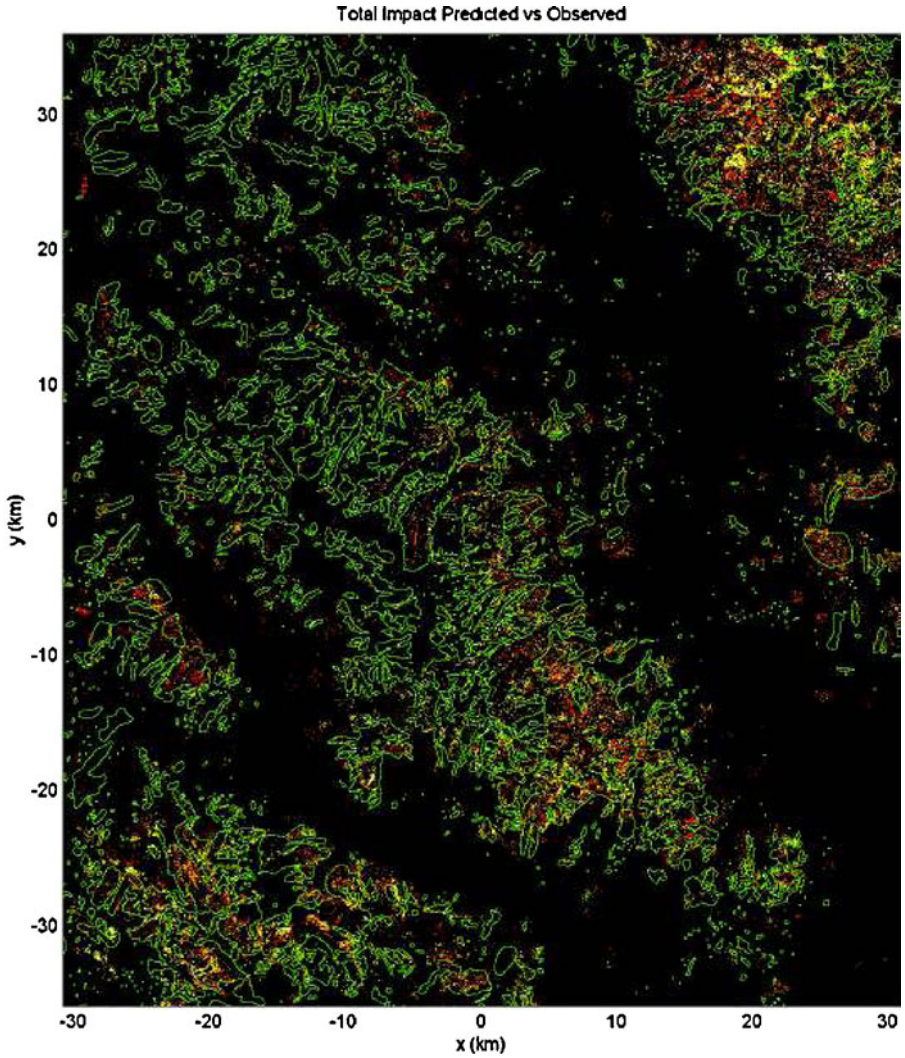

Fig. 4. Density plot of model predictions in the Chelan study area summed across all years, compared with contours of ADS observations likewise summed across all years (1990–2009). Contours of ADS data indicate regions in which ADS observations exceeded one infested tree in a 30 m pixel in some year. Model predictions are rendered in a 'hot' colormap with white saturating at 1000 predicted total MPB-killed trees per hectare and black indicating no MPB impact in any year. Across years and pixels model predictions of presence/absence correlated with observations at $r = 0.7486$.

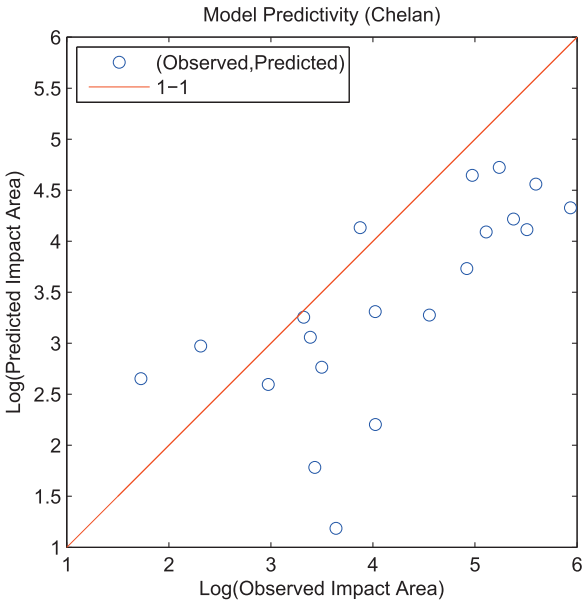

Fig. 5. Comparison of yearly predicted area of impact with observed area of impact in the Chelan study area on a logarithmic scale.

and observations of impact. A confusion matrix, crossing predictions and observations of MPB-impacted and non-impacted grid cells is presented in Table 3. The diagonal elements of the confusion matrix are correct model predictions; off-diagonal elements are either false negatives (lower left) or false positives (upper right). The sum of the diagonal elements divided by the total of all elements is 0.8566, indicating 85.66% accurate predictions. Yearly correspondence between predicted and observed area impacted is compared in Fig. 1. Total net impact across all nine years of prediction and observation is conveyed by the density/contour plot in Fig. 2. To test sensitivity of the correlation coefficients and confusion matrix to spacing/positioning of the error grid the size of error grids was changed both up and down by a factor of two; accuracy measurements were altered by less than one percent. In Fig. 3 growth rate predictions for the spatial model are compared with observations, giving $r^2 = 0.926$.

3.2. Model validation in Chelan study area

Using model parameters estimated for the SNRA study area (see Table 2) and downscaled temperature data the model was applied to the Chelan study area. A confusion matrix, calculated on 0.96 km pixels, indicated a predictivity (fraction of true positive and true negative predictions) of 84.81% (see Table 4). Total net

Table 4
Confusion matrix for model predictions in the Chelan study area, tabulating agreement between model predictions and observations on square 0.9216 km^2 cells from 1990 to 2009. Simulations were run with nominal model parameters (see Table 2). Diagonal elements of the confusion matrix are correct model predictions of either impact or non-impact; the off-diagonal elements are either false negatives (lower left) or false positives (upper right). The ratio of correct to all elements indicates an accuracy of 84.81%, comparable to SNRA study area results.

	Model predicts	
	Non-impacted cell	Impacted cell
Non-impacted cell observed	5467	6759
Impacted cell observed	6913	70,845

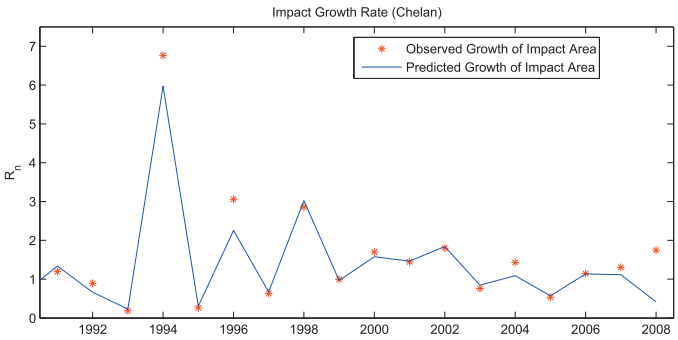

Fig. 6. Comparison of yearly predicted growth rates (solid) with observed growth rates (*) in the Chelan study area, using parameters estimated for the SNRA. The model had $r^2 = 0.9349$.

MPB impact predicted by the model compares favorably with net impact observed (Fig. 4), with overall correlation of 74.86%. While the general outlines of the areas impacted matched up quite well, it is apparent that the model predicted many small spots of infestation inside areas outlined by the ADS observations, resulting in net under-prediction of area impacted by MPB (see Fig. 5). However, the fit of growth rates was excellent, matching almost all the details of the time series with an overall $r^2 = 0.9349$. The exceptional year was 2008, in which predicted growth rates bumped up while observed growth rates bumped down (Fig. 6), potentially due to depletion of susceptible hosts in previous years.

3.3. Model sensitivity

When north bole aspect or air temperatures were used to run the phenology model, the resulting confusion matrices and values of the correlation coefficient differed by less than 1% (Table 5). These results are encouraging and suggest the model can be run using air, rather than phloem temperature. Altering the Allee effect (i.e., A, threshold number of beetles required to overcome tree

Table 5
Results of model sensitivity analysis. Critical model inputs and parameters were altered to assess model sensitivity, including change of study area, thermal inputs, degree to which host density affects beetle movement (μ_1), attack threshold (Allee effect, A) and the number of surviving brood per tree (N). Nominal values are model performance based on MLE estimated values using data from the SNRA study area. Effects on model performance are summarized as predictivity (percentage confusion matrix represented by diagonal), correlation (correlation coefficient of observed and predicted pattern across years on 0.96 km^2 blocks, in percent), and r^2 of the predicted growth rate (fraction of growth rate variance described by model).

Input changed	From	To	Predictivity	Correlation	Growth rate
Nominal values	–	–	85.7	75.0	0.93
Study area	Sawtooth	Chelan	84.8	74.9	0.94
Host density	Observed	Mean	83.0	61.2	0.18
Phloem temperature	South side	North side/ambient	85.1	74.9	0.92
Minimum motility (μ_1)	−10.9	−6	81.6	51.7	0.04
Attack threshold (A)	39.8 MPB/day	100	86.1	76.0	0.91
		10	85.5	74.9	0.92
		0	21.4	14.3	0.32
Surviving brood (N)	2023 MPB/tree	1022	86.4	75.9	0.92
		4046	85.6	75.1	0.92

defenses) had a much larger effect on model accuracy. When the Allee effect was completely removed, model predictivity dropped to less than 21% (Table 5). When the attack threshold was reduced or increased, however, model predictions changed <0.5%, with a slight increase in false positives. Changing the number of beetles that survive to emerge from a tree, N, was similar to altering the attack threshold. Decreasing N by 50% increased model predictivity by approximately 1%, and doubling the number of survivors had no appreciable effect on model accuracy.

Altering host tree density reduced model predictivity to 83% with a much larger reduction in the correlation coefficient and fit between predicted and annual growth rates (Table 5). Most of the loss in predictivity was due to an increase in false negatives from 520 to 1986. Altering beetle motility also decreased all aspects of model accuracy. Changing μ_1 from −10.9 to −6, corresponding to a motility increase from 18.5 to 2480 m^2/day at host densities of 1000 trees/ha, resulted in a reduction in predictivity, the spatial correlation coefficient and fit between predicted and annual growth rates (Table 5). False negatives increased by a factor of five from 520 to 2561, and only 4% of the variance in annual growth rates were described by the model.

4. Discussion and conclusion

We describe an ecological diffusion model that integrates observed host tree density with MPB dispersal across a landscape. The premise of the dispersal model is that MPB leave a patch based on how many live host trees are encountered within the patch, and motility (rate of leaving a patch) decreases exponentially with host tree density. This model is linked with a previously developed model describing temperature-dependent adult emergence timing and an Allee threshold of attacks on trees (Powell and Bentz, 2009), two factors important in successful tree colonization. The integrated model improves upon Powell and Bentz (2009) by providing a spatially explicit representation of MPB impact across a landscape as a function of both host tree density and temperature. The model was parameterized using observed hourly temperature data, and spatially referenced MPB impact data and host tree density during an outbreak in the SNRA, ID. When run in the same landscape where it was parameterized, the model did a good job of capturing the spatial and temporal details of MPB impact (85.67% accuracy). Similar accuracy (84.8%) was obtained when the model was run using data from a different geographic area (i.e., Chelan study area). Predicted annual growth rate of area impacted, a measure of MPB population growth rate in areas of relatively consistent host density, was also highly accurate in both the SNRA (92%) and Chelan (94%) study areas. These results suggest the model is robust, and that our mechanistic description of host-dependent MPB motility is an adequate representation of MPB dispersal across a landscape and during a population outbreak. The model also provides insight into the processes that result in spatial and temporal patterns of MPB-caused tree mortality.

Model-estimated beetle motility rates in pixels of dense host trees (i.e., 1000 trees/ha) was 18.5 m^2/ day, consistent with mark-release-recapture measurements of short distance dispersal during an MPB outbreak in central British Columbia (Safranyik et al., 1992). Short distance dispersal (<100 m) comprises the majority of bark beetle dispersal events, particularly during epidemics (Safranyik et al., 1992; Turchin and Thoeny, 1993; Franklin et al., 2000; Kautz et al., 2011). Long distance dispersal events also occur and can be an important aspect of MPB outbreak progression (Aukema et al., 2008; Chen and Walton, 2011). Model estimates suggest that in the absence of host trees to slow them down, beetles disperse on average 3.79 km^2/day. This motility would allow for the initiation of new patches of mass attacked trees at substantial distances, a phenomenon known to occur for at least some small proportion of a population (Safranyik et al., 1992; Aukema et al., 2008; Robertson et al., 2009).

In a sensitivity analysis, the model was highly sensitive to motility rates and host density across the landscape. When motility within patches of host trees was increased or host tree density was decreased, model accuracy dropped. Given our model assumptions, the two factors are inversely related such that low host density directly results in increased motility. High motility or low density both serve to reduce local beetle abundance and subsequent spot initiation, thereby reducing model accuracy. It is well known that the density and spatial arrangement of host trees is an important component of forest susceptibility to MPB outbreaks (Shore and Safranyik, 1992; Simard et al., 2011; Chapman et al., 2012). We implemented a version of our model with "Fickian" diffusion whereby dispersal was not influenced by host tree density predictions did not correlate with either growth rates or spatial patterns of MPB-caused tree mortality. Combined, these results highlight the importance of host tree density in predicting the spatial and temporal pattern of MPB-caused tree mortality and provide a potential mechanistic role in dispersal across a landscape.

MPB mass attacks occur on a tree when adult emergence is locally synchronized, particularly at low population levels (Bentz et al., in press; Logan and Bentz, 1999). In the model, a threshold number of beetles per day (A = 39.8 MPB/day) are required for a mass attack (Raffa and Berryman, 1983). When this threshold requirement (i.e., Allee effect) was completely removed from the model, model accuracy dropped significantly, although changes to the threshold number of attacks only slightly reduced model accuracy. These results indicate a lack of sensitivity in the model to a particular threshold for successful attacks, although the model is very sensitive to having some kind of threshold. Changing the number of surviving brood that could emerge to attack trees was similar to changing the attack threshold; there was little change in model accuracy. In our simulations, MPB populations were in outbreak phase and temperatures during the study period promoted population survival and success (Régnierè and Bentz, 2007; Powell and Bentz, 2009). A sufficient number of beetles were probably available for mass attacks each year, reducing the effect of the size of the threshold and number of surviving brood in the model. In an area of non-outbreak MPB the model may be more sensitive to the actual threshold or brood survival. While the model threshold is not strictly linear, there is an approximately linear trade-off between emergence and a decreasing attack threshold.

Model accuracy did not differ when phloem temperatures from the north or south bole aspect, or air temperatures were used to run the model. These results were somewhat surprising because Powell and Bentz (2009) found that south bole aspect phloem temperatures provided the best predictions of annual growth rate, using the same model for phenology. Also, using estimated hourly temperatures at the Chelan site, compared to observed hourly temperatures at the SNRA site, did not affect model accuracy. These results suggest that air temperature, rather than phloem temperature, may be sufficient for predicting MPB impact, and that downscaled temperature data provide adequate thermal input for running the integrated model on large landscapes.

At the Chelan study area, although model accuracy was high, the model under-predicted the annual area of impact. Due in part to the diversity of conifers in the Chelan area, including MPB host and non-host trees, the number of small spots identified by ADS observers was higher than in the SNRA where lodgepole pine was predominate (Figs. 2 and 6). At both areas the model was consistently poor at predicting the location of small spots that were not strongly correlated with the location of previous patches. Approximately three quarters (76%) of the false negatives in the confusion matrix are associated with small (<1 ha) spots of fewer than ten

trees in the ADS data. Moreover, model results presented here depended on forcing predictions each year with ADS observations of attacked trees from the previous year. The model did a poor job of predicting the final pattern of MPB-killed trees in 2003 when initiated with the observed spatial pattern of killed trees in 1995 and allowed to run continuously using model output from one year as the input to emergence pattern the subsequent year. These results suggest that the evolution of attack pattern depends strongly on small spots which appear somewhat spontaneously on the landscape. Indeed, this pattern of small spots of bark beetle-infested trees that coalesce through time, potentially through dispersal, was documented for a large MPB outbreak in British Columbia (Aukema et al., 2008) and a spruce beetle (*D. rufipennis* Kirby) outbreak in southern UT (DeRose and Long, 2012). Our model can successfully predict the aggregation and growth of these spots, but misses their inception. Without additional information on factors that influence spot initiation, annual data on spot location is required input to the model. Given this input, however, we feel the model can be used to predict population growth in any phase, including endemic populations scattered across a landscape. One factor that could improve this aspect of the model is the inclusion of behavior-modifying chemicals across a landscape. Previous attempts (Powell et al., 1996) suggest it is unlikely a mechanistic dispersal model that includes chemotactic details can be predictive. Future research should examine pixels with false negatives, and conditions that may influence initiation of small patches. These include elevation and topography (de la Giroday et al., 2011), microclimate, site and soil factors (Kaiser et al., 2012), and presence of other insect and disease populations that can be derived from ADS data.

Our model extends the research of Powell et al. (1996) and Logan et al. (1998), and Aukema et al. (2008) by providing a mechanistic description of the link between motility, dispersal and temperature-dependent phenology that facilitate further positive feedback into the system thereby linking sub populations on a landscape. It is known that temperature can generate spatial synchrony in density-dependent populations over large areas (Liebhold et al., 2004), and can be particularly important in species with long distance dispersal capabilities. Peltonen et al. (2002) suggest that spatial correlation in weather variables was more important than dispersal in describing synchrony in forest insect outbreak data, including MPB, at relatively large scales. Our model provides a mechanistic description of how temperature and dispersal can both play a role in generating spatial synchrony among populations. In MPB, adult emergence exceeding an Allee threshold, which results from critical temperature thresholds for development among life stages, may be one temperature-dependent pathway linking sub-populations, creating spatial synchrony and population growth across a landscape.

Motility that enables dispersal across a landscape can also be considered in the context of resistance to movement. As pointed out by McRae et al. (2008) there is a direct connection between diffusion through patches with varying motility and random-walk movement in a circuit network with varying resistances connecting the patches. Motility within a patch and resistance of the patch to movement are inversely proportional, while resistance and residence time in the patch are proportional. Consequently, parameterizing MPB motility as a function of host density on a landscape is equivalent to determining the resistance structure of the landscape to beetle movement. Therefore, the methods presented here can be applied in resource selection analysis for population movement (Moorcroft, 2012), assessing landscape connectivity (McRae et al., 2008) and determining resistance surfaces for gene flow on landscapes (Spear et al., 2010). For example, our model could provide important insights to the potential spread of MPB eastward across the boreal forests of Canada where host tree density becomes increasingly sparse and fragmented (Safranyik et al., 2010). Low host tree density would directly result in increased MPB motility and potentially greater spread rates than have been encountered in more dense lodgepole pine forests, although our model has not been tested on such a large landscape. Further analyses with the model using additional landscapes and population phases will improve our understanding of mechanisms that connect processes at local and large spatial scales and their role in MPB population outbreak dynamics.

Acknowledgements

We thank Jim Vandygriff for assistance with phloem temperature measurements at both study sites. Tom Edwards gave very helpful advice regarding assessing spatial goodness-of-fit. Péter Molnár and Michael Neubert read and commented on earlier drafts, much to our benefit. Funding was provided by the USDA Forest Service, Western Wildland Threat Assessment Center and National Science Foundation, DEB 0918756.

Appendix A. Phenology model for MPB

In each of eight life stages for MPB we describe the developmental process with an extension of the von Foerster equation (Gilbert et al., 2004),

$$\frac{\partial p_i}{\partial t} + r_i[T(t)]\frac{\partial p_i}{\partial a} = \nu_i \frac{\partial^2 p_i}{\partial a^2}, \tag{3}$$

where $p_i(a, t)$ is the density of individuals of developmental 'age' a in stage i at time t. The age variable, a, is a normalized index of development, e.g., weight gain in larvae, and the developmental process in stage i begins at $a = 0$ and ends with $a = 1$. The median developmental rate for the stage, r_i, depends directly and nonlinearly on temperature, $T(t)$, in the developmental environment of the phloem. The parameter ν_i reflects the variance of the developmental rates in stage i. To predict how the distribution of emergence from one life stage, $p_{i-1}(a = 1, t)$, is mapped to the next, Eq. (3) can be solved using Laplace transforms (Powell and Bentz, 2009) to give

$$p_i(a = 1, t) = \int_0^t p_{i-1}(a = 1, \tau)\frac{1 - r_i[T(t - \tau)]}{\sqrt{4\pi\nu_i(t - \tau)^3}} \times \exp\left[-\frac{\left(1 - \int_\tau^t r_i[T(s)]\,ds\right)^2}{\sqrt{4\nu_i(t - \tau)}}\right] d\tau. \tag{4}$$

Practical evaluation of this equation, driven by hourly temperatures in the phloem of attacked trees, is accomplished via trapezoidal integration over days, aggregated every 24 h into an emergence prediction.

Appendix B. Ecological diffusion and homogenization

Using ecological diffusion, we model the daily dispersing population of MPB, with spatial density $P(x, y, t)$ depending on the spatial coordinates, (x, y), and time during the day, t,

$$\frac{\partial P}{\partial t} = \left(\frac{\partial^2}{\partial x^2} + \frac{\partial^2}{\partial y^2}\right)[\mu(S)P], \tag{5}$$

where μ is the motility of the dispersers leaving a patch of trees with density $S(x, y)$. Daily initial conditions for dispersal on day j in year n are set using a combination of predicted emergence and observed ADS impact,

$$P(x, y, t = 0) = NIE_n(j)(H_n^{\text{obs}} > 0). \tag{6}$$

Here N is the (unknown) number of beetles emerging from a single infested host, $E_n(j)$ is the emergence predicted on day j of year n by the phenology model and I is the impact in observed infested trees/ha. The last, parenthetical term indicates the characteristic function on ADS impact observed in year n (H_n^{obs}, corresponding to trees/ha colonized by MPB in the previous year). The characteristic function gives a value of one in pixels with observed impacts and zero otherwise. We have chosen to assume a constant level of impact because estimated impact densities in the SNRA correlate poorly with ground observations and occasionally exceed estimated numbers of standing trees/ha. By contrast, borders of ADS polygons conform well to host presence as well as field observation. Consequently we have chosen to suppress this additional source of variability and use area impacted as a surrogate for net impact (as in Powell and Bentz, 2009). We choose a reference level of $I = 100$ trees/ha.

Finally, at the end of a day of dispersal, arriving MPB must be converted into attacks on healthy hosts. We assume that chemotaxis allows MPB to focus their efforts on particular hosts within a small, but sub-scale to dispersal, attack radius, r. Thus the number of attacking MPB at a point, (x, y), on the dispersal landscape is $P(x, y, t = 1\text{ day})\pi r^2$. The attackers which successfully colonize are those which exceed attack threshold, A,

$$C(x, y,\ \text{day} = j) = \max(P(x, y, t = 1\text{ day})\pi r^2 - A, 0). \tag{7}$$

At the end of the season (i.e., when $E_n(j)$ falls to zero) successful colonizers can be converted to a density of infested trees predicted for the subsequent year,

$$H_{n+1}^{\text{pred}}(x, y) = \min\left[\alpha \sum_j C(x, y, j), S(x, y)\Delta x\Delta y\right] \frac{1}{\Delta x\Delta y}. \tag{8}$$

The minimization accommodates the finite capacity of hosts to accept beetles; only $1/\alpha$ beetles 'fit' in an individual host, and the total number of colonized trees cannot exceed the number of susceptible hosts in a pixel, $S(x, y)\Delta x\Delta y$. This prediction for impact will be compared to ADS observations for the next year, $H_{n+1}^{\text{obs}}(x, y)$.

To speed up solutions we use the method of homogenization, which is derived for the ecological diffusion equation by Garlick et al. (2011). Essentially, rather than solve (5) directly we solve instead

$$\frac{\partial c}{\partial t} = \overline{\mu}\left(\frac{\partial^2 c}{\partial x^2} + \frac{\partial^2 c}{\partial y^2}\right), \tag{9}$$

where $\overline{\mu}$ is the harmonically averaged motility,

$$\overline{\mu}(x, y) = \left(\frac{1}{||\Omega(x, y)||}\int\int_{\Omega(x,y)} \frac{dx'\,dy'}{\mu(x', y')}\right)^{-1},$$

$\Omega(x, y)$ is a rectangular region centered at the point (x, y), and $||\Omega(x, y)||$ is the area of the region of integration. The dependent variable, c, is related to the density of dispersing MPB by

$$c = \mu(x, y)\ \ P(x, y, t).$$

While the homogenized equation (9) is superficially similar to the original dispersal equation (5), c and the diffusion parameter ($\overline{\mu}$) vary on kilometer scales (as opposed to 30 m scales).

Appendix C. Likelihood function and MLE

Given uncertainties in impact intensity and location of ADS polygon boundaries, we have chosen to match observed and predicted areas on scales larger than the 30 m pixel size of the data, but still small enough to resolve relevant patterns. Let (xe_j, ye_k), $1 \le j \le J$, $1 \le k \le K$ be the centers of a uniform grid with spacing Δxe, $\Delta ye = 480$m in the x and y directions, respectively. For each such error cell we define observed impact for year n to be

$$O_{j,k}^n = \int_{-\Delta ye/2}^{\Delta ye/2}\int_{-\Delta xe/2}^{\Delta xe/2} (H_n^{\text{obs}}(xe_j + \xi, ye_k + \eta) > 0)\,d\xi\,d\eta \tag{10}$$

(using the convention that "$(z > 0)$" is one when $z > 0$ and zero otherwise), and the corresponding predicted impact to be

$$I_{j,k}^n = \int_{-\Delta ye/2}^{\Delta ye/2}\int_{-\Delta xe/2}^{\Delta xe/2} (H_n^{\text{pred}}(xe_j + \xi, ye_k + \eta) > 0)\,d\xi\,d\eta. \tag{11}$$

Assuming that errors are normal with mean zero and unknown (but constant) variance σ^2, the negative log likelihood in year n is

$$NLL_n = \frac{1}{2\sigma^2}\sum_{j=1}^{J}\sum_{k=1}^{K}(O_{j,k}^n - I_{j,k}^n)^2 + \frac{JK}{2}\log(2\pi\sigma^2). \tag{12}$$

The total negative log likelihood to be minimized over years of available data (1995–2003) is

$$L(\mu_0, \mu_1, \beta_1, \beta_2) = \sum_{n=1995}^{2003} NLL_n. \tag{13}$$

The search for minima of L was accomplished using a gradient-free simplex search implemented using the `fminsearch` command in MATLAB.

References

Addison, A.L., Powell, J.A., Six, D.L., Moore, M., Bentz, B.J., 2013. The role of temperature variability in stabilizing the mountain pine beetle-fungus mutualism. Journal of Theoretical Biology 335, 40–50.

Alfaro, R., Campbell, R., Vera, P., Hawkes, B., Shore, T., 2004. Dendroecological reconstruction of mountain pine beetle outbreaks in the Chilcotin Plateau of British Columbia. In: Shore, T.L., Brooks, J.E., Stone, J.E. (Eds.), Mountain Pine Beetle Symposium: Challenges and Solutions. Natural Resources Canada, Information Report BC-X-399, pp. 245–256.

Amman, G.D., Cole, W.E., 1983. Mountain pine beetle dynamics in lodgepole pine forests, Part II: population dynamics. USDA Forest Service, GTR-INT-145, pp. 59.

Aukema, B.H., Carroll, A.L., Zheng, Y., Zhu, J., Raffa, K.F., Moore, R.D., Stahl, K., Taylor, S.W., 2008. Movement of outbreak populations of mountain pine beetle: influences of spatiotemporal patterns and climate. Ecogeography 31, 348–358.

Aukema, B.H., Carroll, A.L., Zhu, J., Raffa, K.F., Sickley, T.A., Taylor, S.W., 2006. Landscape level analysis of mountain pine beetle in British Columbia, Canada: spatiotemporal development and spatial synchrony within the present outbreak. Ecography 29, 427–441.

Bentz, B.J., Vandygriff, J.C., Jensen, C., Coleman, T., Maloney, P., Smith, S., Grady, A., Lagenheim, G., 2013. Mountain pine beetle voltinism and life history characteristics across latitudinal and elevational gradients in the western United States. Forest Science (in press).

Bentz, B.J., Bracewell, R.B., Mock, K.E., Pfrender, M.E., 2011. Genetic architecture and phenotypic plasticity of thermally-regulated traits in an eruptive species, *Dendroctonus ponderosae*. Evolutionary Ecology 25 (6), 1269–1288.

Bentz, B.J., Régnierè, J., Fettig, C.J., Hansen, E.M., Hayes, J.L., Hicke, J.A., Seybold, S.J., 2010. Climate change and bark beetles of the western United States and Canada: direct and indirect effects. BioScience 60 (8), 602–613.

Bentz, B.J., 2006. Mountain pine beetle population sampling: inferences from Lindgren pheromone traps and tree emergence cages. Canadian Journal of Forest Research 36 (2), 351–360.

Bentz, B.J., Mullins, D.E., 1999. Ecology of mountain pine beetle (Coleoptera: Scolytidae) cold hardening in the intermountain west. Environmental Entomology 28 (4), 577–587.

Bentz, B.J., Powell, J.A., Logan, J.A., 1996. Localized Spatial and Temporal Attack Dynamics of the Mountain Pine Beetle (*Dendroctonus ponderosae*) in Lodgepole Pine. USDA/FS Research Paper INT-RP-494, December 1996.

Bentz, B.J., Logan, J.A., Amman, G.D., 1991. Temperature dependent development of the mountain pine beetle (Coleoptera: Scolytidae), and simulation of its phenology. Canadian Entomologist 123, 1083–1094.

Berryman, A.A., Dennis, B., Raffa, K.F., Stenseth, N.C., 1985. Evolution of optimal group attack, with particular reference to bark beetles (Coleoptera: Scolytidae). Ecology, 898–903.

Bjornstad, O.N., Peltonen, M., Liebhold, A.M., Baltensweiler, W., 2002. Waves of larch budmoth outbreaks in the European Alps. Science 298, 1020–1023.

Blackard, J.A., Finco, M.V., Helmer, E.H., Holden, G.R., Hoppus, M.L., Jacobs, D.M., Lister, A.J., Moisen, G.G., Nelson, M.D., Riemann, R., Ruefenacht, B., Salajanu, D., Weyermann, D.L., Winterberger, K.C., Brandeis, T.J., Czaplewski, R.L., McRoberts,

R.E., Patterson, P.L., Tycio, R.P., 2008. Mapping U.S. forest biomass using nationwide forest inventory data and moderate resolution information. Remote sensing of Environment 112, 1658–1677.
Biesinger, Z., Powell, J., Bentz, B., Logan, J., 2000. Direct and indirect parametrization of a localized model for the mountain pine beetle–lodgepole pine system. Ecological Modelling 129 (2-3), 273–296.
Boone, C.K., Keefover-Ring, K., Mapes, A.C., Adams, A.S., Bohlmann, J., Raffa, K.F., 2013. Bacteria associated with a tree-killing insect reduce concentrations of plant defense compounds. Journal of Chemical Ecology 39, 1003–1006.
Boone, C.K., Aukema, B.H., Bohlmann, J., Carroll, A.L., Raffa, K.F., 2011. Efficacy of tree defense physiology varies with bark beetle population density: a basis for positive feedback in eruptive species. Canadian Journal of Forest Research 41, 1174–1188.
Borden, J.H., Ryker, L.C., Chong, L.J., Pierce, H.D., Johnston, B.D., Oehlschlage, A.C., 1987. Response of the mountain pine beetle, *Dendroctonus ponderosae*, to five semiochemicals in British Columbia lodgepole pine forests. Canadian Journal of Forest Research 17, 118–128.
Chapman, T.B., Veblen, T.T., Schoennagel, T., 2012. Spatiotemporal patterns of mountain pine beetle activity in the southern Rocky Mountains. Ecology 93, 2175–2185.
Chen, H., Walton, A., 2011. Mountain pine beetle dispersal: spatiotemporal patterns and role in the spread and expansion of the present outbreak. Ecosphere 2 (6), 1–17.
Crabb, B.A., Powell, J.A., Bentz, B.J., 2012. Development and assessment of 30-m pine density maps for landscape-level modeling of mountain pine beetle dynamics. In: Res. Pa RMRS-RP-96WWW. U.S. Department of Agriculture, Forest Service, Rocky Mountain Research Station, Fort Collins, CO, pp. 43.
Cullingham, C.I., Cooke, J.E., Dang, S., Davis, C.S., Cooke, B.J., Coltman, D.W., 2011. Mountain pine beetle host-range expansion threatens the boreal forest. Molecular Ecology 20 (10), 2157–2171.
de la Giroday, H.C., Carroll, A.L., Lindgren, B.S., Aukema, B.H., 2011. Incoming! Association of landscape features with dispersing mountain pine beetle populations during a range expansion event in western Canada. Landscape Ecology 26, 1097–1110.
DeRose, J.R., Long, J.N., 2012. Factors influencing the spatial and temporal dynamics of Engelmann spruce mortality during a spruce beetle outbreak on the Markagunt Plateau, Utah. Forest Science 58, 1–14.
Evenden, J.C., Gibson, A.L., 1940. A destructive infestation in lodgepole pine stands by the mountain pine beetle. Journal of Forestry 38, 271–275.
Franklin, A.J., Debruyne, C., Grégoire, J., 2000. Recapture of Ips typographus L.(Col., Scolytidae) with attractants of low release rates: localized dispersion and environmental influences. Journal of Agricultural Entomology 2, 259–270.
Garlick, M.J., Powell, J.A., Hooten, M.B., Macfarlane, L., 2011. Homogenization of large scale movement models in ecology. Bulletin of Mathematical Biology 73, 2088–2108.
Geiszler, D.R., Gallucci, V.F., Gara, R.I., 1980. Modeling the dynamics of mountain pine beetle aggregation in a lodgepole pine stand. Oecologia 46, 244–253.
Gilbert, E., Powell, J.A., Logan, J.A., Bentz, B.J., 2004. Comparison of three models predicting developmental milestones given environmental and individual variation. Bulletin of Mathematical Biology 66, 1821–1850.
Halsey, R., 1998. Aerial detection survey metadata for the Intermountain Region 4. U.S. Department of Agriculture Forest Service, Forest Health Protection.
Heavilin, J., Powell, J., 2008. A novel method for fitting spatio-temporal models to data, with applications to the dynamics of Mountain Pine Beetle. Natural Resource Modelling 21, 489–524.
Heavilin, J., Powell, J.A., Logan, J.A., 2007. Development and parametrization of a model for bark beetle disturbance in lodgepole forest. In: Miyanishi, K., Johnson, E. (Eds.), Plant Disturbance Ecology. Academic Press, NY, USA, pp. 527–553.
Hughes, R.R., 1973. Dendroctonus: production of pheromones and related compounds in response to host monoterpenes. Zeitschrift für Angewandte Entomologie 73, 294–312.
Jenkins, J.L., Powell, J.A., Logan, J.A., Bentz, B.J., 2001. Low seasonal temperatures promote life cycle synchronization. Bulletin of Math Biology 63, 573–595.
Kaiser, K.E., McGlynn, B.L., Emanuel, R.E., 2012. Ecohydrology of an outbreak: mountain pine beetle impacts trees in drier landscape positions first. Ecohydrology, http://dx.doi.org/10.1002/eco.1286.
Kane, J.M., Kolb, T.E., 2010. Importance of resin ducts in reducing ponderosa pine mortality from bark beetle attack. Oecologia 164, 601–609.
Kautz, M., Dworschak, K., Gruppe, A., Schopf, R., 2011. Quantifying spatio-temporal dispersion of bark beetle infestations in epidemic and non-epidemic conditions. Forest Ecology and Management 262, 598–608.
Lewis, M.J., 2011. Modeling Phloem Temperatures Relative to Mountain Pine Beetle Phenology. Utah State University (MS Thesis), http://digitalcommons.usu.edu/gradreports/60
Liebhold, A., Koenig, W.D., Bjornstad, O.N., 2004. Spatial synchrony in population dynamics. Annual Review of Ecology, Evolution, and Systematics 35, 467–490.
Littell, J.S., Elsner, M.M., Mauger, G.S., Lutz, E., Hamlet, A.F., Salathé, E., 2011. Regional Climate and Hydrologic Change in the Northern US Rockies and Pacific Northwest: Internally Consistent Projections of Future Climate for Resource Management, Project report: April 17, 2011. Latest version online at http://cses.washington.edu/picea/USFS/pub/Littell_etal_2010/
Logan, J.A., Powell, J.A., 2001. Ghost forests, global warming, and the mountain pine beetle (Coleoptera: Scolytidae). American Entomologist 47 (3), 160–173.
Logan, J.A., Bentz, B.J., 1999. Model analysis of mountain pine beetle (Coleoptera: Scolytidae) seasonality. Environmental Entomology 28 (6), 924–934.
Logan, J.A., White, P., Bentz, B.J., Powell, J.A., 1998. Model analysis of spatial patterns in mountain pine beetle outbreaks. Theoretical Population Biology 53 (3), 236–255.
McCambridge, W.F., 1967. Nature of induced attacks by the Black Hills beetle, *Dendroctonus ponderosae* (Coleoptera: Scolytidae). Annals of the Entomological Society of America 64, 534–535.
McGregor, M.D., 1978. Status of mountain pine beetle Glacier National Park and Glacier View Ranger District, Flathead National Forest, MT, 1977. Forest Insect and Disease Management Report No. 78-6, Missoula, MT.
McRae, B.H., Dickson, B.G., Keitt, T.H., Shah, V.B., 2008. Using circuit theory to model connectivity in ecology, evolution and conservation. Ecology 89, 2712–2724.
Meddens, A.J.H., Hicke, J.A., Ferguson, C.A., 2012. Spatiotemporal patterns of observed bark beetle-caused tree mortality in British Columbia and the western United States. Ecological Applications 22, 1876–1891.
Mitchell, R.G., Preisler, H.K., 1991. Analysis of spatial patterns of lodgepole pine attacked by outbreak populations of the mountain pine beetle. Forest Science 37 (5), 1390–1408.
Moorcroft, P.R., 2012. Mechanistic approaches to understanding and predicting mammalian space use: recent advances, future directions. Journal of Mammology 93, 903–916.
Nathan, R., Perry, G., Cronin, J.T., Strand, A.E., Cain, M.L., 2003. Methods for estimating long-distance dispersal. Oikos 103, 261–273.
Peltonen, M., Liebhold, A.M., Bjornstad, O.N., Williams, D.W., 2002. Spatial synchrony in forest insect outbreaks: roles of regional stochasticity and dispersal. Ecology 83 (11), 3120–3129.
Perkins, D.L., Swetnam, T.W., 1996. A dendroecological assessment of whitebark pine in the Sawtooth-Salmon River region, Idaho. Canadian Journal of Forest Research 26, 2123–2133.
Pfeifer, E.M., Hicke, J.A., Meddens, A.J.H., 2011. Observations and modeling of aboveground tree carbon stocks and fluxes following a bark beetle outbreak in the western United States. Global Change Biology 17, 339–350.
Pierce, K.B., Ohmann, J.L., Wimberly, M.C., Gregory, M.J., Fried, J.S., 2009. Mapping wildland fuels and forest structure for land management: a comparison of nearest neighbor imputation and other methods. Canadian Journal of Forest Research 39, 1901–1916.
Pitman, G.B., 1971. Trans-verbenol and alpha-pinene: their utility in manipulation of the mountain pine beetle. Journal of Economic Entomology 64, 426–430.
Powell, J.A., Bentz, B.J., 2009. Connecting phenological predictions with population growth rates for mountain pine beetle, an outbreak insect. Landscape Ecology 24, 657–672.
Powell, J., Jenkins, J., Logan, J., Bentz, B.J., 2000. Seasonal temperature alone can synchronize life cycles. Bulletin of Mathematical Biology 62, 977–998.
Powell, J.A., Logan, J.A., Bentz, B.J., 1996. Local projections for a global model of mountain pine beetle attacks. Journal of Theoretical Biology 179 (3), 243–260.
Preisler, H.K., Hicke, J.A., Ager, A.A., Hayes, J.L., 2012. Climate and weather influences on spatial temporal patterns of mountain pine beetle populations in Washington and Oregon. Ecology 93, 2421–2434.
Raffa, K.F., Powell, E.N., Townsend, P.A., 2012. Temperature-driven range expansion of an irruptive insect heightened by weakly coevolved plant defense. Proceedings of the National Academy of Science 110, 2193–2198.
Raffa, K.F., Aukema, B.H., Bentz, B.J., Carroll, A.L., Hicke, J.A., Turner, M.G., Romme, W.H., 2008. Cross-scale drivers of natural disturbances prone to anthropogenic amplification: dynamics of biome-wide bark beetle eruptions. BioScience 58 (6), 501–518.
Raffa, K.F., Aukema, B.H., Erbilgin, N., Klepzig, K.D., Wallin, K.F., 2005. Chapter four interactions among conifer terpenoids and bark beetles across multiple levels of scale: an attempt to understand links between population patterns and physiological processes. Recent Advances in Phytochemistry 39, 79–118.
Raffa, K.F., Berryman, A.A., 1983. The role of host plant resistance in the colonization behavior and ecology of bark beetles (Coleoptera: Scolytidae). Ecological Monographs 53, 27–49.
Rasmussen, L.A., 1974. Flight and attack behavior of mountain pine beetles in lodgepole pine of northern Utah and southern Idaho. USDA For. Serv. Res. Note INT-180.
Régnière, J., Powell, J., Bentz, B., Nealis, V., 2012. Effects of temperature on development, survival and reproduction of insects: experimental design, data analysis and modeling. Journal of Insect Physiology 58, 634–647.
Régnierè, J., Bentz, B.J., 2007. Modeling cold tolerance in the mountain pine beetle, *Dendroctonus ponderosae*. Journal of Insect Physiology 53 (6), 559–572.
Robertson, C., Nelson, T.A., Jelinski, D.E., Wulder, M.A., Boots, B., 2009. Spatial–temporal analysis of species range expansion: the case of the mountain pine beetle, *Dendroctonus ponderosae*. Journal of Biogeography 36 (8), 1446–1458.
Robertson, C., Nelson, T.A., Boots, B., 2007. Mountain pine beetle dispersal: the spatial–temporal interaction of infestations. Forestry Science 53, 395–405.
Safranyik, L., Carroll, A.L., Régnière, J., Langor, D.W., Riel, W.G., Shore, T.L., Peter, B., Cooke, B.J., Nealis, V.G., Taylor, S.W., 2010. Potential for range expansion of mountain pine beetle into the boreal forest of North America. The Canadian Entomologist 142, 415–442.
Safranyik, L., Carroll, A., 2006. The biology and epidemiology of the mountain pine beetle in lodgepole pine forests. In: Safranyik, L., Wilson, B. (Eds.), The mountain pine beetle: a synthesis of biology, management, and impacts on lodgepole pine. Natural Resources Canada, Canadian Forest Service, Victoria, BC, Canada, pp. 3–66.

Safranyik, L., Linton, D.A., Silversides, R., McMullen, L.H., 1992. Dispersal of released mountain pine beetles under the canopy of a mature lodgepole pine stand. Journal of Applied Entomology 113, 441–450.

Safranyik, L., Silversides, R., McMullen, L.H., Linton, D.A., 1989. An empirical approach to modeling local dispersal of the mountain pine beetle (*Dendroctonus ponderosae*) in relation to sources of attraction, wind direction, and speed. Journal of Applied Entomology 108, 498–511.

Safranyik, L., 1978. Effects of climate and weather on mountain pine beetle populations. In: Berryman, A.A., Amman, G.D., Stark, R.W. (Eds.), Proceedings of Symposium on Theory and Practice of Mountain Pine Beetle Management in Lodgepole Pine Forests, April 25–27, 1978. Washington State University, Pullman, Washington, pp. 77–84.

Safranyik, L., Shrimpton, D.M., Whitney, H.S., 1975. An interpretation of the interaction between lodgepole pine, the mountain pine beetle and its associated blue stain fungi in western Canada. In: Baumgartner, D.M. (Ed.), Management of Lodgepole Pine Ecosystems: Symp. Proc. Washington State Univ. Cooperative Extension Service. , pp. 406–428.

Sambaraju, K.R., Carroll, A.L., Zhu, J., Stahl, K., Moore, R.D., Aukema, B.H., 2012. Climate change could alter the distribution of mountain pine beetle outbreaks in western Canada. Ecography 35, 211–223.

Shore, T., Safranyik, L., 1992. Susceptibility and risk rating systems for the mountain pine beetle in lodgepole pine stands. Forestry Canada, Pacific and Yukon Region, BC-X-336.

Simard, M., Powell, E.N., Raffa, K.F., Turner, M.G., 2011. What explains landscape patterns of tree mortality caused by bark beetle outbreaks in Greater Yellowstone? Global Ecology and Biogeography 21, 556–567.

Spear, S.F., Balkenhol, N., Fortin, M-J., McRae, B.H., Scribner, K., 2010. Use of resistance surfaces for landscape genetic studies: considerations for parameterization and analysis. Molecular Ecology 19, 3576–3591.

Turchin, P., 1998. Quantitative Analysis of Movement. Sinauer Associates, Inc., Sunderland, MA.

Turchin, P., Thoeny, W., 1993. Quantifying dispersal of southern pine beetles with mark-recapture experiments and a diffusion model. Ecological Applications 3, 187–198.